Electronic Supplementary Material (ESI) for Nanoscale.
This journal is © The Royal Society of Chemistry 2017

Supplementary Material

Au@PdO$_x$ with PdO$_x$-rich shell and Au-rich core embedded in Co$_3$O$_4$ nanorods for catalytic combustion of methane

Nating Yang [a,b] Jingwei Liu,[a] Yuhan Sun,[a,c] and Yan Zhu [a,c] *

[a] CAS Key Laboratory of Low-Carbon Conversion Science and Engineering, Shanghai Advanced Research Institute, Chinese Academy of Sciences, Shanghai 201210, China

[b] University of Chinese Academy of Sciences, Beijing 100049, China

[c] School of Physical Science and Technology, ShanghaiTech University, Shanghai 201210, China

Catalysts preparation

$Co(Ac)_2{\cdot}4H_2O$ (5×10^{-3} mol) was dissolved in ethylene glycol (15 mL) at 80 °C under vigorous stirring and argon flow. Na_2CO_3 aqueous solution (0.2 M, 50 mL) was then added to the mixture dropwise and purple precipitate was gained, which was further aged for 5~10 minutes at 80 °C. 10 mL aqueous solution of K_2PdCl_4 ($0\sim11.7\times10^{-3}$ M) and $AuCl_3$ ($0\sim4.1\times10^{-3}$ M) with certain weight ratio of Pd to Au (5:1, 3:1, 2:1, or 1:2) was then added to the aforementioned solution. The resulting solution was further aged at that temperature for 1.5 h and then transferred to Teflon lined stainless steel autoclave (100 mL) at 160 °C for 3 h. After the reaction, the dark purple solid precipitate was separated by centrifugation and washed with water and ethanol. After that the precipitate was dried at 60 °C in vacuum, and then calcined in air at 300 °C for 3 h. The weight loading of the noble metal for the four samples are in the range of 2.76-2.93 wt%, and the corresponding weight ratios of Pd to Au are detected as 5:1, 3.4:1, 2.4:1, and 1:1.5, respectively.

The Co_3O_4 nanorods were prepared based on the above synthesis without the addition noble metal. 2.45% Pd/Co_3O_4 nanorods and 2.79% Au/Co_3O_4 nanorods were respectively prepared in the same procedure with the addition of K_2PdCl_4 or $AuCl_3$. Au-Pd (5:1)/Co_3O_4 nanorods were prepared by loading Au-Pd nanoparticles on the Co_3O_4 nanorods: K_2PdCl_4, $AuCl_3$, and PVA (Pd/Au/PVA mass ratio = 5:1:10) were dispersed in H_2O, which was set in an ice bath under vigorous stirring for 15 min. Then, a desired amount of 0.1 mol/L$NaBH_4$ aqueous solution was quickly added into the above solution, generating a brown Au-Pd colloidal solution. Finally, a certain amount of the Co_3O_4 nanorods was added into the Au-Pd colloidal solution (theoretical Au–Pd loading = 3 wt %). After 6 h of stirring, the mixture was washed, dried, and calcined in air at 300 °C for 3 h.

Characterization

Powder X-ray diffraction (XRD) patterns of the samples were recorded on an Ultima IV, performed with Cu Ka radiation (1.5418 Å). The transmission electron microscopy (TEM), high-angle annular dark-field scanning TEM (HAADF-STEM) and element mapping images were acquired from using the transmission electron microscope (Tecnai G2 F20 S-Twin, FEI) equipped with energy dispersive X-ray spectroscopy (EDS) at an accelerating voltage of 200 kV. The binding energies of the surface species on the catalysts were determined by X-ray photoelectron spectroscopy (XPS) (Thermo Scientific K-Alpha) using Al Kα (hν = 1486.6 eV) as the excitation source. Correction of the charge effect was made with the C (1s) peak at 284.8 eV. The surface atomic ratios were calculated by correcting the intensity with theoretical sensitivity factors based on the Scofield cross-section. Peak decomposition was performed using the Avantage software from Thermo with a Smart background subtraction and 30%/70% Lorentizian/Gaussian peak shape. The noble metal loadings were measured by the inductively coupled plasma atomic emission spectroscopic (ICP-AES) technique on a PerkinElmer Optima 8000 spectrometer. The N_2 sorption experiments were done with physical adsorption analyzer (TriStar II 3020, Micromeritics). All the samples were degassed at 200 °C for 6 h under vacuum prior to measurement. The surface areas were calculated using the Brunauer−Emmett−Teller (BET) method. Methane temperature-programmed reduction (CH_4-TPR) experiments were carried out on a chemical adsorption analyzer (Autochem II 2920, Micromeritics). Before Temperature program reduction (TPR) measurement, 50 mg catalyst was pretreated in an air flow at 300 °C for 2 h. After cooled to 60 °C, the sample was exposed to a flow (50 $mL\cdot min^{-1}$) of 10 vol. % CH_4 and 90 vol. % He mixture and kept at 60 °C for 1 h, finally the sample was heated from 60 to 800 °C at a ramp of 10 $°C\cdot min^{-1}$ in the CH_4-He mixture flow. The CO chemisorption on the catalysts was tested by volumetric chemisorptions, which were carried out on the Micromeritics AutoChem II 2920. All catalysts were reduced in hydrogen at 473 K for 30 min and then flushed with He carrier gas at this temperature for 30 min. After cooling to 323 K in He flow, 5% CO/He (0.5173 mL) was dosed 20 times in He flow. The metal dispersion was calculated on the basis of the CO−metal chemisorption stoichiometry of 1

Catalytic test

The catalytic performance of the catalysts for methane combustion was measured in a fixed bed quartz tubular reactor (internal diameter=5 mm, length=500 mm) at atmospheric pressure. All the catalysts for evaluating were pelletized, crushed, and sieved to 40-60 mesh. The catalysts (100 mg) were packed between two layers of quartz wool, and the reagent gas mixture (1 vol.% CH_4, 10 vol.% O_2, and 89 vol.% N_2) with a flow rate of (100 $mL\cdot min^{-1}$) was led over the catalysts, thus the reactor space velocity (SV) was maintained at 60000 $mL\cdot g^{-1}\cdot h^{-1}$. The temperature was increased stepwise from 20 to 450 °C or 500 °C at a ramp of 5 $°C\cdot min^{-1}$. The reaction products were analyzed by micro gas chromatograph (INFICON 3000) equipped with MS5A and Plot Q columns (for separation of H_2, CO, N_2, CO_2, O_2, CH_4, C_2H_4, and C_2H_6) and TCD detector. During the whole test period, carbon dioxide and water are the only reaction products detected.

To investigate the catalytic performance of the catalysts for wet methane combustion and the mixed gases similar to the exhaust of lean-burn natural gas engine, 5-10 vol. % of water vapour was introduced by a calibrated water pump and vaporized in the heated gas feed line before entering the reactor. 50 $mL\cdot min^{-1}$ of reagent gas mixture was led over the 100 mg of catalysts and the SV was maintained at 30000 $mL\cdot g^{-1}\cdot h^{-1}$.

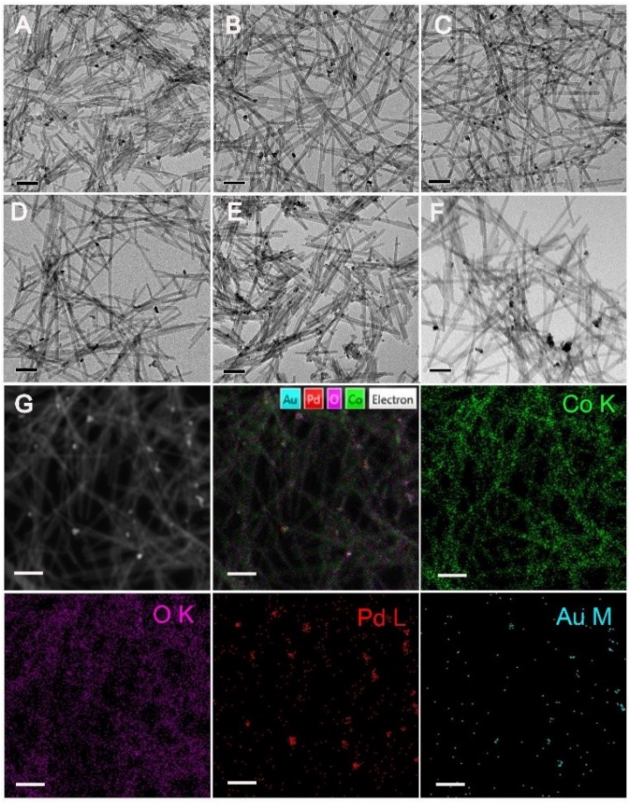

Figure S1. TEM images of (A) Pd-Au (5:1), (B) Pd-Au (3:1), (C) Pd-Au (2:1), (D) Pd-Au (1:2), (E) Pd, and (F) Au on cobalt hydroxycarbonate, respectively. The scale bars are 50 nm. (G) HAADF-STEM and elemental mapping images of Pd-Au (3:1)/ cobalt hydroxycarbonate and the scale bars are 40 nm.

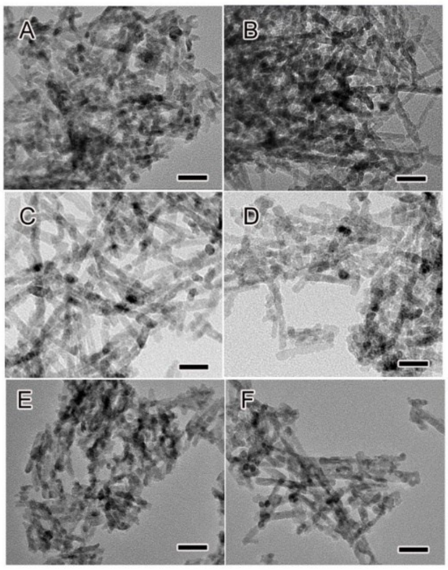

Figure S2. TEM images of (A) Au@PdO_x (1:5)/Co_3O_4, (B) Au@PdO_x (1:3)/ Co_3O_4, (C) Au@PdO_x (1:2)/Co_3O_4, (D) Au@PdO_x (2:1)/ Co_3O_4, (E) Pd/Co_3O_4, and (F) Au /Co_3O_4. The scale bars are 25 nm.

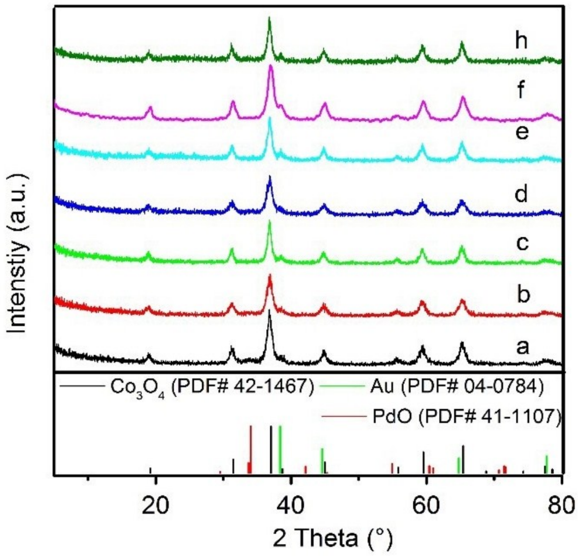

Figure S3. XRD patterns of (a) Pd/Co_3O_4, (b) $Au@PdO_x$ (1:5)/Co_3O_4, (c) $Au@PdO_x$ (1:3)/ Co_3O_4, (d) $Au@PdO_x$ (1:2)/Co_3O_4, (e) $Au@PdO_x$ (2:1)/Co_3O_4, (f) Au/Co_3O_4, and (h) Au-Pd (5:1)/Co_3O_4.

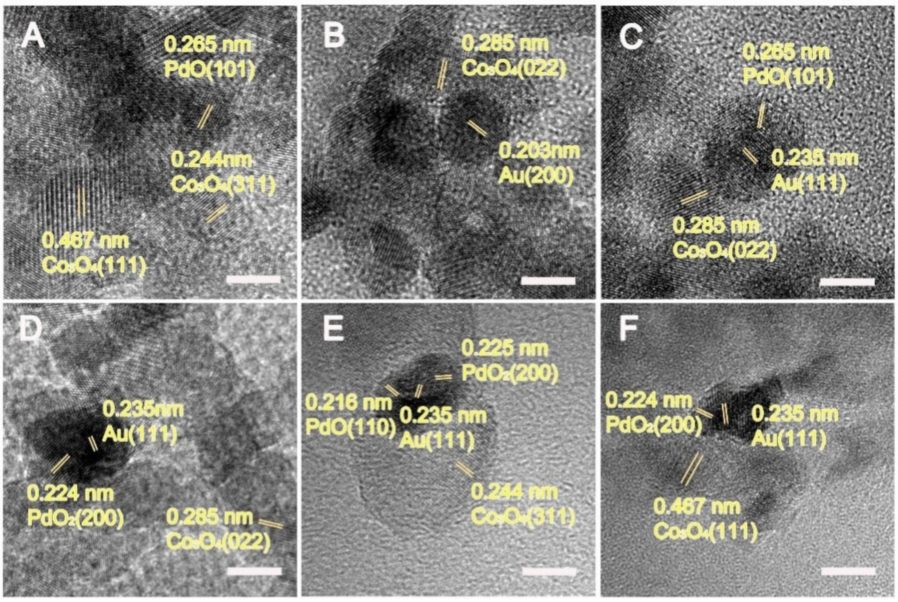

Figure S4. HRTEM images of (A) Pd/Co_3O_4, (B) Au/Co_3O_4, (C)$Au@PdO_x$ (1:5)/Co_3O_4, (D) $Au@PdO_x$ (1:3)/Co_3O_4, (E)$Au@PdO_x$ (1:2)/Co_3O_4, (F)$Au@PdO_x$ (2:1)/Co_3O_4, the scale bars are 4 nm.

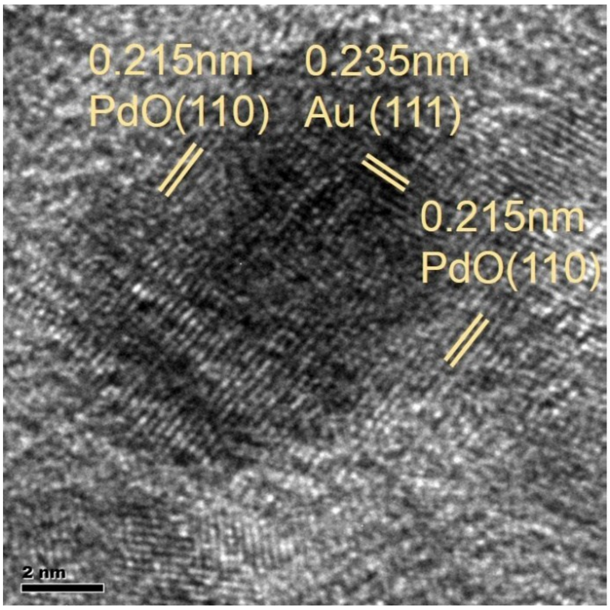

Figure S5. HRTEM image of Au@PdO$_x$ (1:5)/Co$_3$O$_4$.

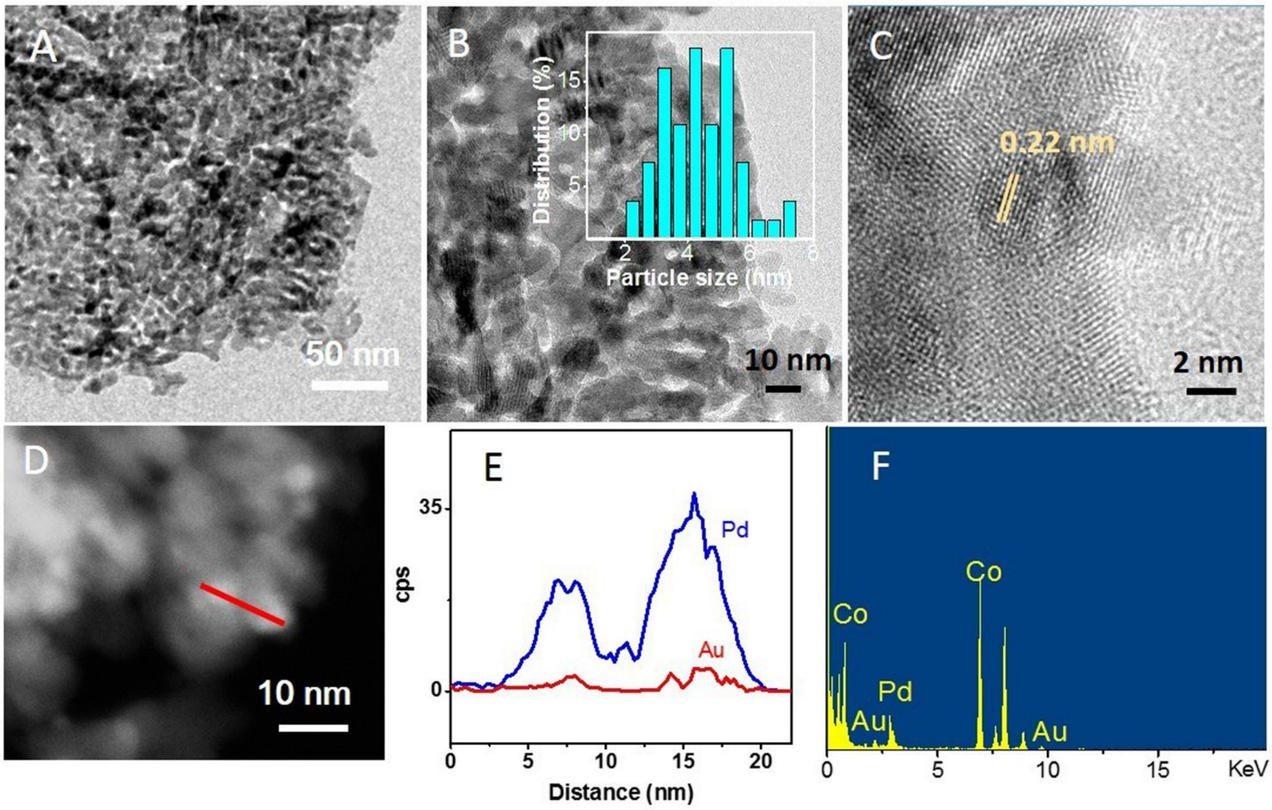

Figure S6. (A-B) TEM images of AuPd(1:5)/Co$_3$O$_4$, the insert of (B) is the size distribution of the bimetallic nanoparticles, (C) HRTEM image of AuPd nanoparticles, (D-E) HAADF-STEM and the line scanning profiles of AuPd nanoparticle and (F) the corresponding EDS spectra.

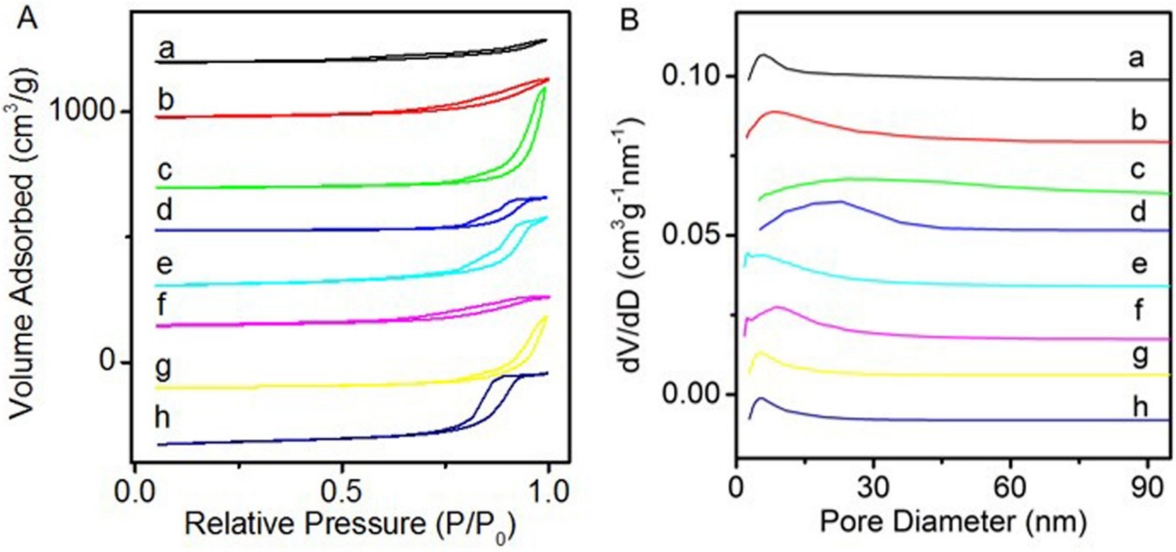

Figure S7. (A) Nitrogen adsorption–desorption isotherms and (B) pore size distribution of the catalysts: (a) Au@PdO$_x$ (1:5)/ Co_3O_4, (b) Au@PdO$_x$ (1:3)/ Co_3O_4, (c) Au@PdO$_x$ (1:2)/ Co_3O_4, (d) Au@PdO$_x$ (2:1)/ Co_3O_4, (e) Au-Pd (1:5)/Co_3O_4, (f) Pd/Co_3O_4, (g) Au/ Co_3O_4, and (h) Co_3O_4.

Figure S7 shows the N_2 adsorption–desorption isotherms and pore-size distributions of the samples. All of the samples displayed a type III isotherm with a hysteresis loop in the relative pressure range of 0.5–1.0 (Figure S7A), indicating the weak interaction between the sample and the N_2 and the generation of mesopores in the samples resulted from the stacking of the nanorods. The pore-size distributions of the samples are in the ranges of 10-38 nm (Figure S7 B). As shown in Table 1 and Table S1, the BET surface areas of Au/Co_3O_4, Pd/Co_3O_4, Au@PdO$_x$/Co_3O_4, and AuPd/Co_3O_4 were in the ranges of 60.0–80.1 m^2/g, much lower than that of Co_3O_4 (111.4 m^2/g).

Table S1. BET specific surface area (S_{BET}) and the specific reaction rates of the catalysts for methane oxidation at 250 °C.

Catalysts	S_{BET} ($m^2 \cdot g^{-1}$)	r $\mu mol \cdot m^{-2}_{cat} \cdot s^{-1}$	Catalysts	S_{BET} ($m^2 \cdot g^{-1}$)	r $\mu mol \cdot m^{-2}_{cat} \cdot s^{-1}$
AuPd (1:5)/Co_3O_4	80.1	1.26	Au@PdO_x (1:5)/Co_3O_4	65.5	2.96
Pd/Co_3O_4	67.8	1.04	Au@PdO_x (1:3)/Co_3O_4	79.6	1.90
Au/Co_3O_4	71.7	1.04	Au@PdO_x (1:2)/Co_3O_4	68.7	1.84
Co_3O_4	111.4	0.23	Au@PdO_x (2:1)/Co_3O_4	60.0	1.10

Table S2. Au and Pd weight loading of the samples calculated from ICP-AES, BET specific surface area (S_{BET}) from N_2 absorption isotherms, CO chemical adsorption amounts (CAA), adsorbed oxygen/lattice oxygen molar ratio (O_{ads}/O_{latt}), Pd^{x+}/Pd^0 molar ratio ($x \geq 2$), reaction rate (r) (calculated by weight amount of the catalysts) and TOF (calculated by CO CAA) at 250 °C, apprent activation energy (E_a), and the temperatures for 10 % and 90 % conversion of methane (T_{10} and T_{90}).

Catalysts	Au content (wt %)	Pd content (wt %)	S_{BET} ($m^2 \cdot g^{-1}$)	CO CAA ($\mu mol \cdot g^{-1}$)	O_{ads}/O_{latt} molar ratio	Pd^{x+}/Pd^0 molar ratio	r ($\mu mol \cdot g^{-1} \cdot s^{-1}$)	TOF (s^{-1})	E_a ($kJ \cdot mol^{-1}$)	T_{10} (^oC)	T_{90} (^oC)
Au@PdO_x (1:5)/Co_3O_4	0.49	2.44	65.5	92.8	0.51	29.3	194	2.09	50.9	210	344
Au@PdO_x (1:3)/Co_3O_4	0.63	2.13	79.6	122.5	0.43	25.7	151	1.23	63.7	226	358
Au@PdO_x (1:2)/Co_3O_4	0.81	1.96	68.7	116.6	0.41	24.3	126	1.08	62.3	230	378
Au@PdO_x (2:1)/Co_3O_4	1.75	1.18	60.0	70.8	0.40	5.4	66	0.93	62.2	255	449

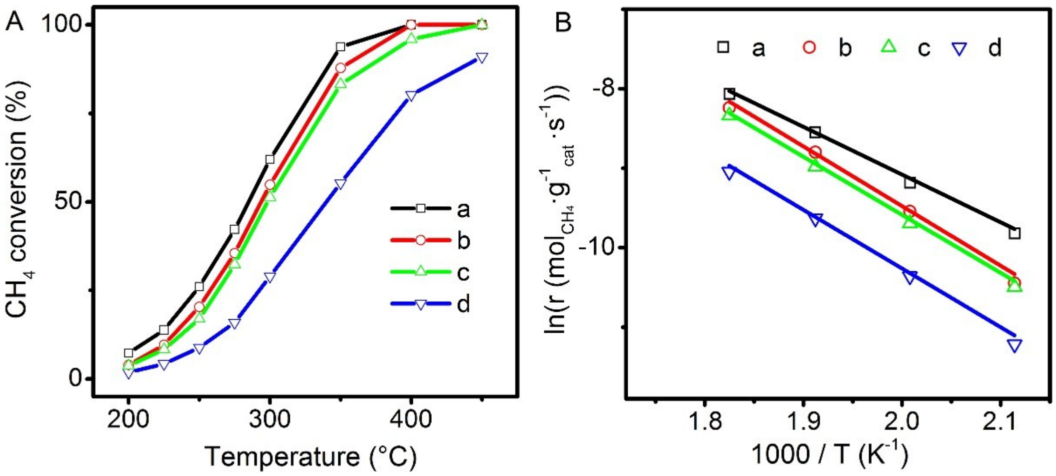

Figure S8 (A) Methane conversion versus temperatures and (B) ln (rate)-1/T plots for CH_4 combustion over (a) Au@PdO_x (1:5)/Co_3O_4, (b) Au@PdO_x (1:3)/Co_3O_4, (c) Au@PdO_x (1:2)/Co_3O_4, (d) Au@PdO_x (2:1)/Co_3O_4, respectively.

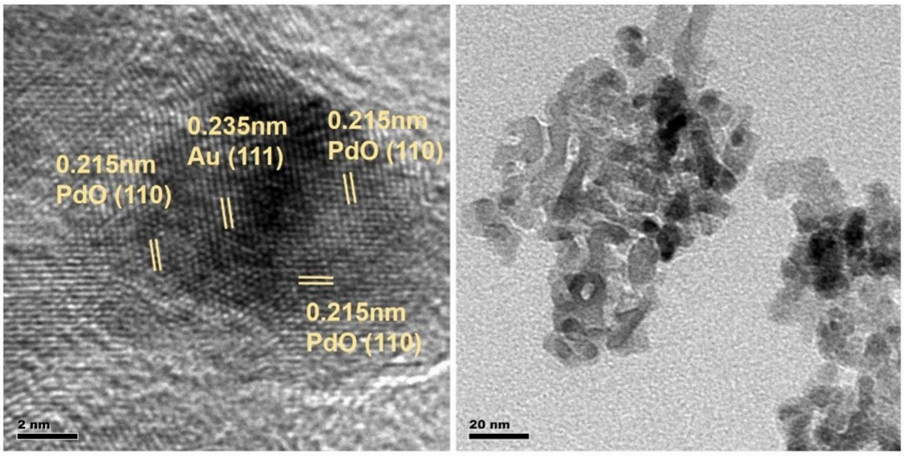

Figure S9. TEM images of the spent Au@PdO_x (1:5)/Co_3O_4 after catalytic reaction.

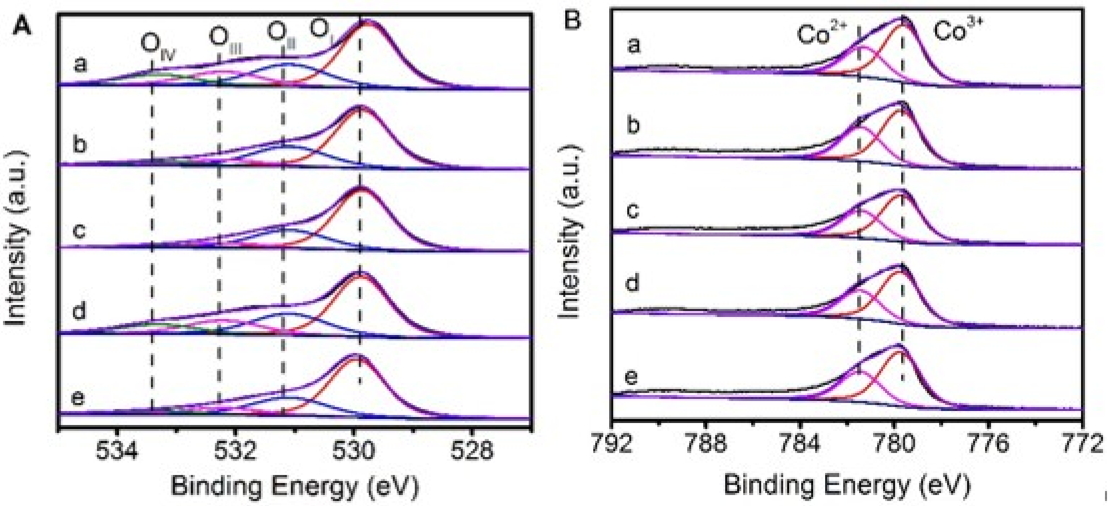

Figure S10. (A) O 1s and (B) Co 2p XPS profiles of the catalysts: (a) Co_3O_4, (b) Pd/Co_3O_4, (c) Au/Co_3O_4, (d) Au@PdO_x (1:5)/Co_3O_4 and (e) AuPd(1:5)/Co_3O_4, respectively.

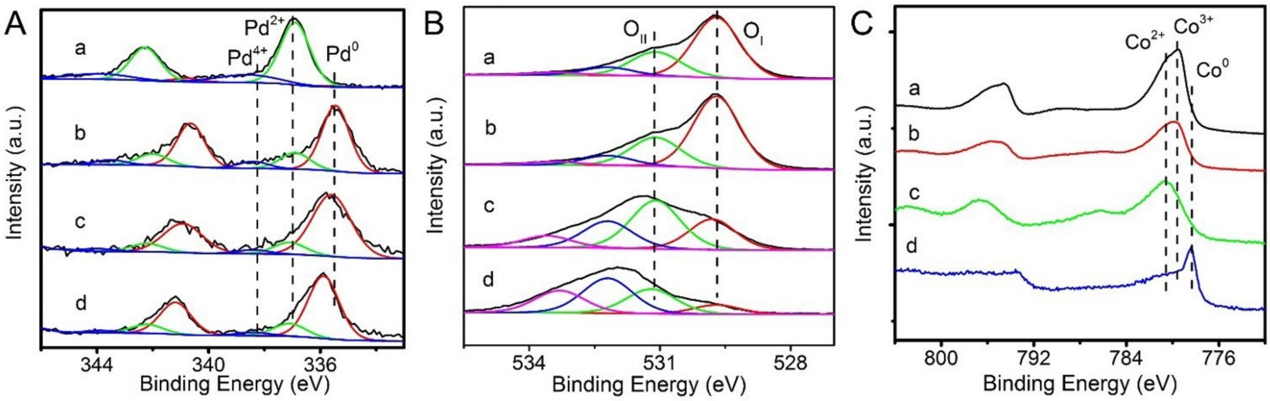

Figure S11. (A) Pd 3d, (B) O 1s, and (C) Co 2p XPS profiles of (a)Au@PdO_x (1:5)/Co_3O_4 and the derivative samples which were treated by CH_4-TPR at different temperature range: (b) 60-300 ^oC, (c) 60-600 ^oC, (d) 60-800 ^oC.

Table S3. Reduction temperature, peak area and percent of adsorbed oxygen and oxygen in PdO_x (O_{ads} (PdO_x)), and lattice oxygen in Co_3O_4 (O_{latt}) in the catalysts calculated from the CH_4-TPR spectra (Figure 5).

Catalysts	O_{ads} (PdO_x)		O_{latt}	
	Peak Center (°C)	Area Fit (ratio)	Peak Center (°C)	Area Fit (ratio)
Au@PdO_x (1:5)/Co_3O_4	272	8.8 (28%)	522	22.6 (72%)
AuPd (1:5)/Co_3O_4	292	9.0 (29%)	481	21.9 (71%)
Pd/Co_3O_4	292	7.3 (31%)	501	16.2 (69%)
Au/Co_3O_4	371	6.2 (18 %)	450	27.2 (82%)
Co_3O_4	323	1.3 (14%)	475	7.9 (86 %)